KONA Powder and Particle Journal

KONA Powder and Particle Journal No. 42 (2025) 227–240/https://doi.org/10.14356/kona.2025002 Original Research Paper

An Empirical Equation for Rapid Validation of the Performance of Commercial N95 Equivalent Respirators†

Sheng-Chieh Chen*, Yu Zhang, Genhui Jing, Peng Wang and Da-Ren Chen

Department of Mechanical and Nuclear Engineering, Virginia Commonwealth University, USA

The COVID-19 pandemic has underscored the importance of wearing effective facepiece filtering respirators (FFRs) to reduce infection and disease transmission. One of the reasons causing the widespread prevalence was found to be the failure of N95-Equivalent FFRs (N95-EFs), i.e., efficiency <<95 %, during the pandemic. To investigate the reasons causing the ineffectiveness of commercial N95-EFs, this study measured the efficiency of several dozens of commercially available N95-EFs following standard testing protocols. The specifications of the N95-EF including fiber diameter, solidity and surface potential of the main layer media of N95-EFs were also determined. We provide a simple method for manufacturers to quickly screen the efficiencies of their N95-EF products before distributing them to the market. We found that the failures of N95-EF are majorly attributed to overprediction of the efficiency due to i) missing neutralization of challenging particles, ii) too small or oversize of challenging particles, and iii) particle detectors with large sizing limits (>500 nm). Based on the pressure drop, respirator area, and surface potential of the N95-EFs, an empirical equation is developed to fast screen and help design effective N95-EFs.

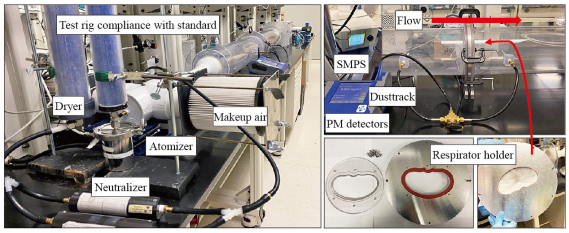

Keywords: COVID-19, N95, facepiece filtering respirators, pressure drop, efficiency, empirical equation

1. Introduction

Since the outbreaks of the COVID-19 pandemic, the novel coronavirus (SARS-CoV-2) has caused nearly a billion infections and 7 million deaths due to its high transmission and severe fatality rate (Dhand and Li, 2020; Jayaweera et al., 2020; Prather et al., 2020; Yan et al., 2018). In addition to contacting surfaces with fomite, SARS-CoV-2 had a high airborne transmission through virus-laden droplets and aerosols, which are released by sneezing, coughing, speaking, and breathing of the infected person. These droplets and aerosols can travel up to 8 m, and the desiccated residue or droplet nuclei may stay suspended for hours (CDC, 2021; Dhand and Li, 2020), which significantly enlarged the transmission rate. To provide protection for individuals and lower the transmission of SARS-CoV-2 through aerosol transmissions, face masks and filtering facepiece respirators (FFRs) are required or highly recommended by the Centers for Disease Control and Prevention, CDC, since the outbreak of COVID-19 in March 2020 (CDC, 2020). N95, KN95, FPP2, and KF94 respirators, etc., whose filtration efficiencies against laboratory-produced NaCl particles are required to be larger than 94–95 %, are commercially available and affordable for the general public. It is of great importance that these N95 Equivalent-Facepiece filtering respirators (N95-EFs) have good quality to protect people from infection and spreading of viruses.

1.1 Failure of FFRs

According to the CDC, approximately 60 % of KN95, the most widely available N95-EFs on the market during the COVID-19 pandemic in 2020 and 2021, did not meet the requirement, i.e., filtration efficiency (FE) ≥95 % (CDC, 2021). Aiming to determine the reasons for the unsatisfactory performance of FFRs or to develop easy screening methods, quite many research teams evaluated commercially available FFRs (e.g., Duncan et al., 2021; Plana et al., 2021; Schilling et al., 2021).

As is known, the standard testing protocols by the National Institute for Occupational Safety and Health (NIOSH) and by the National Standards of the People's Republic of China (GB 2626, 2006) require rigorous procedures and designated or recommended equipment and conditions such as particle type and size distribution, particle charging state, particle detector, filtration flow rate, sample conditioning, environmental control chamber, etc. Because of the strict and time-consuming testing procedures and the expensiveness of the required facilities, any simplifications and noncompliance with the procedures would lead to incorrect filtration efficiency results. Additionally, the urgent demands of tremendous quantities during the early period of the pandemic caused the failures

† Received 11 June 2023; Accepted 11 July 2023
J-STAGE Advance published online 13 January 2024
* Corresponding author: Sheng-Chieh Chen;
Add: 401 West Main St., Richmond, VA, 23284, USA
E-mail: scchen@vcu.edu
FAX: +1-804-827-0306

of quality assurance and control of the N95-EFs by the manufacturers. However, it was very difficult for the public to distinguish between legitimate and counterfeit products. The wearing of counterfeit products would be a reason for speeding the spread of SARS-CoV-2 during the pandemic.

1.2 Reasons for N95-EF failure

The efficiency of N95-EFs was often largely overestimated if standard procedures were not followed. In the evaluations of N95-EFs, the required size distribution, charging state, and deliquesce of challenging particles were often not considered (Cai and Floyd, 2020; Duncan et al., 2021; Patra et al., 2022; Schilling et al., 2021; Stahl et al., 2021). For instance, some researchers did not neutralize the challenging particles, which could lead to the overprediction of the Columbic force and the FE. Because particles will carry a higher mean number of charges after they are aerosolized than the neutralized state, as required. During particle dispersion (e.g., aerosolization by atomizer), a triboelectric or contact charge develops along the particle surface because of mechanical friction from the surface and particle contact. This energy transfer could generate an excess charge of 1~10^5 elementary units (Forsyth et al., 1998). For example, it was found that 200 nm NaCl particles carried a mean elementary charge of ~3.7 compared to ~1.0 charge of neutralized particles (Forsyth et al., 1998). According to the theoretical model (Chang et al., 2016; 2018), the FE for a neutralized 100 nm NaCl particle through a charged filter media (~75 μC/m^2) can be increased from ~60 % to over 95 % if it is not neutralized. This indicates the importance of a completed neutralization before challenging the respirator to prevent a significant overprediction of FE.

While the recommended particle detector by the NIOSH was a mass-based laser light scattering photometer detector having a sizing limit of ~0.1 μm, some researchers applied detectors with a limit larger than 300–500 nm (e.g., optical particle counter), thus, the high penetration from small particles, i.e., <100 nm, was neglected. Indeed, the most penetrating particle size (MPPS) of charged filter media normally falls at 20–50 nm (Chang et al., 2015; Tang et al., 2018a, b, c). The overestimation of EFs becomes more significant when the challenging aerosol particles have a larger number (or count) median diameter (NMD) due to the inherent relatively higher EF of larger particles. For example, the FE of a neutralized 500 nm by charged media could reach ~95 % but it reduced to ~88 % and ~80 % when the size was reduced to 100 nm and 50 nm (MPPS), respectively (Chen et al., 2014). Without taking the high penetration of small particles into account, the overall efficiency was thus overestimated. This analysis also reveals the importance of complying with the specified size distribution of challenging particles by the standards, which was an NMD of 0.075 ± 0.02 μm and geometric standard deviation (GSD) of smaller than 1.86. The more shifting of size distribution to larger size ranges, the more significant overestimation of FE will be. To note, there exists a lack of correspondence between the specified size distribution (NMD ~0.075 μm) and particle detector (>0.1 μm) in the standard, which should be addressed in the future.

The filtration flow rate (or flow face velocity through media) designated by the standards was 85 L/min (or ~10 cm/s face velocity). Some researchers performed the FE test with a face velocity lower than 10 cm/s, especially when a flat sheet of the FFR media instead of a whole FFR was evaluated. For an N95-rated FFR, the FE can increase from ~88 to 95 % for MPPS when reducing the face velocity from 10 to 5 cm/s (Chen et al., 2014). From the foregoing discussion, simplifications and noncompliance with standard methods could produce significant overestimations of FE.

Given the limited access to required facilities and compliance with complex experimental procedures, theoretical models based on the single fiber theory may be applied to predict the FEs (Chang et al., 2016). However, this method can also be problematic as it requires accurate specifications of the FFRs, i.e., fiber diameter, thickness, packing density (solidity), charge density, and face velocity. Among them, charge density is the most inaccessible parameter due to the complexity of charge figuration and its measurement. Thus, it is commonly seen that an estimated value of charge density was used in the calculation to match experimental FE data (Balazy et al., 2006; Chang et al., 2016; Hao et al., 2021). However, the empirically-theoretically fitted charging density is accurate only when other filter parameters are correctly determined. Even if other parameters are correct, an incorrect charging density may be obtained if any filtration equations for each deposition mechanism are incorrect, typically occurring for the equation of electrostatic deposition.

For a good preparation for future respiratory pandemics, it is urgent to develop a fast, convenient, and accurate method for manufacturers and certification laboratories to quickly qualify and prove the effectiveness of N95-EFs before distributing them to the market. Using a modified three-layer model based on the measured and calculated particle depositions through the cracks, researchers successfully developed an empirical equation to predict the penetration rate of outdoor particles into buildings (Chen et al., 2012; You et al., 2012). Similarly, an empirical equation model combining experimental data and filtration theory and describing the relationship between variables is a potentially useful method to quickly provide reliable predictions and insights into the performance of N95-EFs.

1.3 Objectives

In this study, a rigorous test rig and strict measurement procedure in compliance with Chinese Standard GB 2626

(GB 2626, 2006) were applied to measure the efficiency of 50 different commercial N95-EFs. The GB 2626 method was chosen because it was similar to the NIOSH standard and the majority (30 out of 50) of the tested respirators were KN95. In addition to the mass-based FE by a photometer, the number-based size-fractioned FE was also determined by a scanning mobility particle sizer (SMPS, Model 3938, TSI Inc., Shoreview, MN) for the 50 N95-EFs. In addition to the FE, the thickness, fiber size, solidity and surface potential of main filtration layer were measured. The charge density of N95-EF media was obtained by comparing the experimental and theoretical efficiency according to Chang et al. (2016). The correlation between calculated charging density and surface potential was investigated. If a good linear correlation is seen, the easily accessible surface potential can substitute the charging density as a representative filtration parameter.

This study is trying to develop an empirical equation to predict the FEs of N95-EFs. Because FEs are size-dependent and number-based according to filtration theory (Hinds, 1999), the FE for MPPS measured by SMPS was selected as the target. The N95-EF can pass the evaluation if its FE at MPPS is higher than 95 %. The qualified N95-EF thus has a minimum FE of 95 % against any size of particles.

Considering many filter parameters that cannot be easily obtained, including solidity, charging density, and fiber diameter, they may be excluded from the empirical equation. Instead, three easily accessible but essential parameters, including pressure drop, mask area, and surface potential, should be good representative variables of FE at MPPS and be applied in the empirical equation. The pressure drop of the respirator is the product of fiber diameter, solidity,, and thickness; thus, it should be an important parameter of FE. Since most N95-EFs are charged, the feasibility of using the surface potential in the empirical equation will be investigated. The respirator area was included because under a constant testing flow rate of 85 L/min, the face velocity and thus the FE would vary significantly. In fact, the area varies largely for commercial N95-EFs.

The developed equation will be evaluated by comparing its predictions with the experimental efficiency of MPPS particles. The model will be further validated by predicting the FE for 5 extra N95-EF samples. The final goal of this study is to provide this validated equation and its constraints for the use of manufacturers or certified laboratories to quickly qualify N95-EFs to secure their quality.

2. Materials and methods

2.1 N95-EF sources and selection

The N95-EFs evaluated in this study included N95, KN95, KF94, and FFP2 respirators purchased from Amazon, Costco Wholesale, Walmart, Kroger, and CVS. A total of 50 samples were collected and investigated for their FEs and specifications. Before the FE measurement, the first examination was to check their appearance. Samples that appeared to have any damage, deformation and defects on the surface were excluded. Besides, those N95-EFs containing both nanofiber and microfiber layers (by SEM analysis) were also removed because their FE could not be easily predicted by filtration theory. Moreover, samples were also excluded when the variation of FEs for 5 randomly picked respirators from the same box (usually sold with 20–50 packs per box) was too significant. For example, when one standard derivation of FE (the measurement method will be shown later) from 5 samples was higher than 20 % of average efficiency. A high deviation means their average FEs were not statistically significant to be adopted. Finally, a total of 15 samples were excluded from the first examination.

Among the qualified 35 N95-EFs, the evaluation results of 30 samples were used to develop the empirical equation for predicting the FE at MPPS. The rest 5 samples were used to validate the equation. All samples were measured with their thickness, solidity (packing density), fiber diameter, filtration area, charge density and pressure drop. To note, some N95-EFs contain more than one charged (major) layer, so the above specifications should be determined based on all charged layers.

2.2 Thickness

The thickness of the main filter layer (excluding the top and bottom layers having very coarse fibers without charges, for support only) was measured by a digital caliper with a resolution of 0.001 mm. To increase the accuracy, 5 pieces of the main layer cut from different locations were combined for their average thickness. The measurement was repeated for 5 runs for 5 respirators from the same box to obtain the representative thickness.

2.3 Solidity

Solidity was obtained by taking the ratio of the fiber volume to the total volume of the main filtration layer (usually meltblown of polypropylene) of the respirator. The total volume was determined by the product of media thickness and sample size (cut with 40 mm in diameter). The volume of the filtration layer was determined from the ratio of their weight to the sample volume. The solidity, α, is calculated as:

$$\alpha = \frac{W / \rho_f}{t \times \pi \times 4^2 / 4} \quad (1)$$

where W is the weight of the flat sheet [g], ρ_f is the density of the filter media (0.855 g/cm^3 for polypropylene) and t is the thickness.

The fiber diameter applied in this study was the effective fiber diameter based on the solidity and pressure drop measured (Davies, 1973). Chang et al. (2016) have proven that

effective fiber diameter was applicable and suitable for the prediction of FE using single fiber efficiency theory.

2.4 Filtration area

In the determination of total filtration area of N95-EFs that exhibited different shapes and sizes, a simple method was developed. First, the pressure drop for the whole respirator under 85 L/min was measured. Then, a flat circular sheet of 4 cm in diameter (or 12.56 cm^2) was cut from the respirator and measured for its pressure drop under 10 cm/s (or 7.54 L/min). The pressure drop is linearly increased with face velocity for the same filter media. If the measured pressure drop of the whole respirator is $P1$ and that of the 4 cm circular sheet is $P2$, the area of the whole respirator, A, is calculated as:

$$\frac{P1}{P2}=\frac{85/A}{7.54/12.56}\Rightarrow A=\frac{141.6\times P2}{P1} \tag{2}$$

2.5 Theoretical filtration efficiency

The theoretical single fiber efficiency model was developed to predict the FE of both charged (or electret) and uncharged (or mechanical) filter media under clean conditions (Chang et al., 2016; Hinds, 1999). It is widely applied, and here we summarize the models that can accurately predict the FEs for researchers' reference (Chang et al., 2016, 2018; Liu et al., 2023; Tien et al., 2020). The theoretical particle penetration, P_{theo}, is calculated as (Bahk et al., 2013; Hinds, 1999; Wang et al., 2007, 2011):

$$P_{theo}=\exp\left(-\frac{4\alpha E_T t}{\pi d_f(1-\alpha)}\right) \tag{3}$$

where d_f is the fiber diameter in the filter media and E_T is the total single fiber efficiency due to diffusion (E_D), interception (E_R), interception of diffusing particles (E_{DR}), impaction (E_I), and electrostatic attraction (E_q), and determined as:

$$E_T=1-(1-E_D)(1-E_R)(1-E_{DR})(1-E_I)(1-E_q) \tag{4}$$

The E_D, E_R, E_{DR} and E_I are calculated as (Wang et al., 2007; 2011):

$$E_D=0.84Pe^{-0.43} \tag{5}$$

$$E_R=\frac{1+R}{2Ku}\left[2\ln(1+R)-1+\alpha+\left(\frac{1}{1+R}\right)^2\left(1-\frac{\alpha}{2}\right)-\frac{\alpha}{2}(1+R)^2\right] \tag{6}$$

$$E_{DR}=\frac{1.24R^{2/3}}{(Ku\times Pe)^{1/2}} \tag{7}$$

$$E_I=\frac{1}{(2Ku)^2}\left[(29.6-28\alpha^{0.62})R^2-27.5R^{2.8}\right]Stk \tag{8}$$

where Pe is the Peclet number, Ku is the Kuwabara hydrodynamic parameter, R is the ratio of particle to the fiber diameter, and Stk is the Stokes number. The Pe, Ku, and Stk are calculated as:

$$Pe=\frac{d_f U_0}{D} \tag{9}$$

$$Ku=\frac{-\ln\alpha}{2}+\alpha-\frac{\alpha^2}{4}-\frac{3}{4} \tag{10}$$

$$Stk=\frac{\rho_p d_x^2 C_c U_0}{18\mu d_f} \tag{11}$$

where U_0 is face velocity, D is the diffusion coefficient, ρ_p is NaCl density (2.2 g/cm^3), d_x is particle diameter, C_c is the Cunningham slip correction factor (Hinds, 1999) and μ is the air viscosity (N·s/m^2). In **Eqn. (4)**, E_q can be further calculated according to the depositions by the Coulombic force $E_{qC}(n)$ and that by the dielectric polarization force E_{qD}, as:

$$E_q=1-[1-E_{qC}(n)](1-E_{qD}) \tag{12}$$

where $E_{qC}(n)$ is the function of the number of charges, and n, is the number of charges the particles carried. The $E_{qC}(n)$ and E_{qD} can be calculated as (Chang et al., 2015):

$$E_{qC}(n)=\left(\frac{1-\alpha}{Ku}\right)^{1/8}\frac{\pi N_{CD}}{1+2\pi N_{CD}^{1/4}} \tag{13}$$

and

$$E_{qD}=\left(\frac{1-\alpha}{Ku}\right)^{2/5}\frac{\pi N_{DD}}{1+2\pi N_{DD}^{2/3}} \tag{14}$$

N_{CD} and N_{DD} are dimensionless parameters for charged and uncharged particles through bipolarly charged fibrous filter media, respectively, and defined as:

$$N_{CD}=\frac{C_c\sigma q(n)}{3\pi\mu\varepsilon_0(1+\varepsilon_f)d_x U_0} \tag{15}$$

and

$$N_{DD}=\frac{2C_c\sigma^2 d_x^2}{3\mu\varepsilon_0(1+\varepsilon_f)^2 d_f U_0}\left(\frac{\varepsilon_p-1}{\varepsilon_p+2}\right) \tag{16}$$

where σ is the charging density of the fiber (C/m^2), $q(n)$ is the carried charges of the particle with d_x (C), ε_f is the fabric dielectric constant (1.5 for the polypropylene), ε_0 is the permittivity of the vacuum (8.85×10^{-12} $C^2/N\cdot m^2$) and ε_p is the relative permittivity of the particle which is 4.86 for NaCl.

By considering the charge distributions of particles (size dependent) through charged filter media, the size dependent penetration, $P_{theo,dx}$, is calculated as:

$$P_{\text{theo},dx} = \sum_{n=-10}^{n=10} f(n) \times \exp\left(-\frac{4\alpha E_T(n)t}{\pi d_f(1-\alpha)}\right),$$

n includes 0 (17)

where $f(n)$ is the fraction of the d_x particles that carry number of n charges and the total efficiency E_T is rewritten to consider particle charges (up to 10 elementary charges) as:

$$E_T(n) = 1-(1-E_D)(1-E_R)(1-E_{DR})(1-E_I)\left[1-E_{qC}(n)\right]\left(1-E_{qD}\right) \quad (18)$$

To note, **Eqn. (17)** considers the polarization depositions for both neutral (zero charge) and charged particles, which resulted in an agreement between the model prediction and experimental data (Chang et al., 2016). Without considering the polarization deposition for charged particles, it would lead to errors. **Eqn. (17)** considers particle charges up to with 10 elementary charges, but normally the particle concentration fractions reduce to negligible (<1 %) for more than 6 charges for submicron particles (<1 μm).

From **Eqns. (3)** to **(18)**, the theoretical EF is size dependent, $\eta_{\text{theo},dx}$ and calculated as:

$$\eta_{\text{theo},dx} = 1 - P_{\text{theo},dx} \quad (19)$$

The result of **Eqn. (19)** will be compared with the size fractioned efficiency determined by the SMPS (detailed in **Section 2.7**).

As shown above, to predict the efficiency of charged filter media using the theoretical model involves many equations and cumbersome calculations, which can easily cause errors. The charge density in **Eqns. (15, 16)** was not easily and accurately measured. Thus, one can extrinsically determine it by fitting a value of the charging to match the size fractioned efficiency curve between the theoretical calculation and experimental measurement (Chang et al., 2016). However, an accurate charging density can be obtained only if accurate experimental data are obtained and all required parameters presented in these equations are correctly measured and determined. This study intended to determine the empirical charging density of each respirator investigated, so the calculations were inevitable. To conclude, given the complexity of obtaining the theoretical efficiency, charge density, and all filter specifications, it is necessary to find an easily accessible method to quickly screen the effectiveness and FE of respirators.

2.6 Surface potential measurement

A Trek model 244A electrostatic voltmeter equipped with a 1017AE probe (Advanced Energy Industries, Inc., Denver, CO) was used to measure the dipolar surface potential of the main filtration layer, as shown in **Fig. 1**. This voltmeter uses a technique that nullifies the field between the probe and the filter (Antoniu et al., 2011; Sachinidou et al., 2018). The potential V_p of the voltmeter probe is driven by the electronic circuitry of the instrument at the potential V of the monitored surface ($V_p = V$). Thus, the electric field in the air gap between the sample and probe is nullified. This measurement configuration is equivalent to that of a capacitor calculated as:

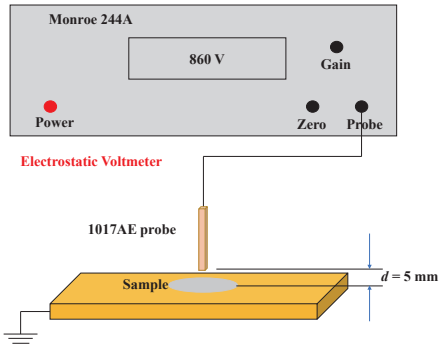

Fig. 1 Schematic of surface potential measurement by electrostatic voltmeter.

$$C_p = \frac{Q}{V} = \frac{\varepsilon_d A}{t} \quad (20)$$

where C_p is the capacitance of the capacitor, Q is the charge carried by the surface area A of the sample surface, V is the measured surface potential (i.e., a potential difference between the sensor and the tested surface), ε_d is the permittivity of the sample between the electrode and the tested surface, and t is the thickness of the sample (Kachi et al., 2011). The surface electric charge density σ, assumed to be uniformly distributed, can be expressed as (Kachi et al., 2011):

$$\sigma = \frac{V\varepsilon_d}{t} \quad (21)$$

During the surface potential measurement, the major layer was positioned onto a grounded metal plate and a noncontact probe of the electrostatic voltmeter was placed 5 mm above the layer surface, according to Kachi et al. (2011). The environmental relative humidity (RH) was controlled between 30 % and 50 % to minimize the effect of RH on charge dissipation during the measurement (Kachi et al., 2011). The samples were in circular shape with a diameter of 4 cm. To obtain representative results, 20 different spots on the surface of the sample were measured and averaged. To be mentioned, dragging the sample and causing friction with the surface should be avoided during measurements, which can generate static charges. The measurements were repeated for 5 different pieces from different respirator samples in the same box to provide the average and standard deviation.

The measured surface potentials were correlated with the obtained charged density from theoretical calculations.

2.7 Filtration efficiency measurement

The standard GB 2626 method was applied to determine the performance of N95-EFs. Before the FE measurement, temperature and humidity conditioning were conducted. That is, 5 samples from a box were pretreated with temperature and RH at 38 ± 2.5 °C and 85 ± 5 %, respectively, for 24 ± 1 hours. Then, they were conditioned under 70 ± 3 °C and RH <30 % in a forced air oven for other 24 ± 1 hours. Finally, they were treated under –30 ± 3 °C in the freezer for other 24 ± 1 hours. We randomly picked 10 samples to conduct the conditioning test.

The mass-based FE, η_m, based on the upstream, $C_{m,up}$, and downstream mass concentrations, $C_{m,down}$, of NaCl particles of the respirator under 85 L/min flow rate, was determined as:

$$\eta_m = 1 - \frac{C_{m,down}}{C_{m,up}} \tag{22}$$

The mass concentrations were measured by a TSI DustTrak DRX (Model 8533, TSI Inc., Shoreview, MN) photometer. The challenging particles required a specific size distribution having a NMD of 0.075 ± 0.02 μm and a geometric standard deviation (σ_g) less than 1.86. **Fig. 2** shows an example of the size distribution of the generated particles in this study.

The TSI 8130 Automated Filter Tester (TSI Inc., Shoreview, MN) is a standard reference test rig. It uses a laser with a wavelength of 780 nm to illuminate challenging particles and to detect light scattering for the upstream and downstream particles of the filter by photometers. Lights scattered from particles whose diameters are much smaller than the wavelength of the incident laser would be very weak ($\propto d_x^6$), so the sensitivity is largely reduced for small particles. Therefore, photometric measurement is largely biased toward the detection of larger particles in the distribution, and it can significantly overestimate the FE of the filter media, typically against the small challenging particles (**Fig. 2**, by the SMPS) for charged media. Therefore, to provide the worst performance of respirator, the FE at MPPS, η_{MPPS}, which is the number-based minimum efficiency is measured. To find η_{MPPS}, the largest size dependent penetration, $P_{largest,dx}$, should be calculated by taking the ratio of upstream, $C_{n,up}$, to downstream number concentration, $C_{n,down}$, of the respirator as:

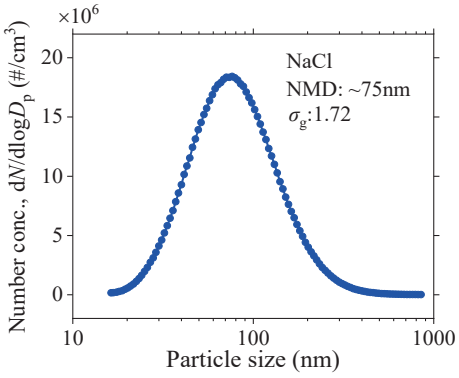

Fig. 2 Size distribution of challenging particles.

$$\eta_{MPPS} = 1 - P_{largest,d_x} = 1 - \frac{C_{n,down}}{C_{n,up}} \tag{23}$$

The size distribution shown in **Fig. 3** is the denominator in **Eqn. (23)**. The experimental setup for mass-based and number-based FE measurements is shown in **Fig. 3**.

To measure the number-based filtration efficiency, the TSI SMPS (Model 3938, TSI Inc., Shoreview, MN) was applied, and the procedures are the same as that of the mass-based testing procedure by Dusttrak. Before introducing challenging particles into the respirator, they should be totally neutralized by a neutralizer, Po-210 here, which depends on the resident time (or flow rate) and ion concentration (Hinds, 1999). It is worth mentioning that since the efficiency testing was under a flow rate of 85 L/min, the upstream concentration of the particle source at smaller particle size may be low, which can lead to inaccuracy of EF of MPPS (usually in 20–50 nm for charged media). Thus, a suitable atomizer that has a sufficiently high flow rate (dilution rate can be reduced) and high particle concentration as well as the required size distribution is essential. In this study, a homemade atomizer with a maximum flow rate of 8 L/min was applied. The concentration of NaCl solution was 0.5–1.5 wt% in this study. To obtain representative results, measurements for the filtration efficiency by every type of FFRs were repeated at least five times using new samples.

3. Results and discussion

3.1 Specification of studied N95-EFs

3.1.1 Mass- and Number-Based FE

This study found that pretreatment with temperature and humidity did not change the FE results of the tested respirators. **Table 1** summarizes the specifications and FE data measured for the first 30 tested respirators, including mass- and number-based efficiency, MPPS, pressure drop, filtration area, thickness, effective fiber diameter, solidity, empirical charging density, and surface potential. The order of these respirators shown in the table was based on their mass-based efficiency from high to low. It is seen 9 out of 30 did not pass 0.95 (or 95 %) mass-based efficiency. The pass rate shown here is reasonable because the half of them were purchased after January 2022, so only ~30 % failed. Due to the small size distribution of the NaCl challenging particles and more sensitivity of SMPS than the Dusttrak, as expected, the number-based efficiency was lower than that of mass-based ones except for samples 11, 16 and 21. These three respirators, in general, had a high pressure drop (150–225 Pa, oriented toward mechanical filter) and medium charging density (MPPS not small), causing a higher efficiency toward small sizes. A total of 11 out of 30 tested

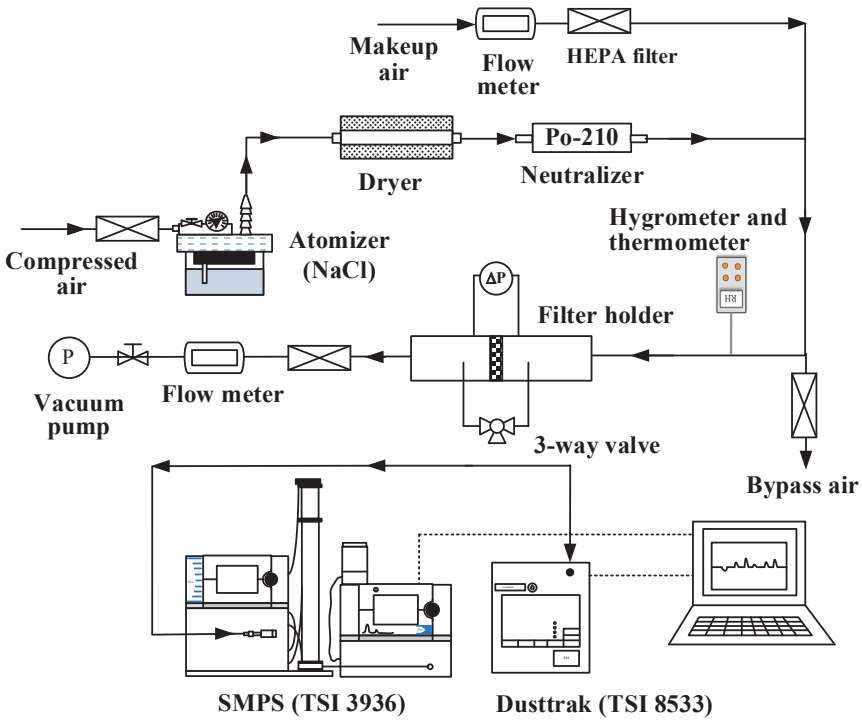

Fig. 3 Test rig for measuring both mass- and number-based FEs of N95-FEs.

respirators did not pass the 95 % number-based efficiency. Samples 8, 17 and 20 passed mass-based FE while failed for number-based FE. Nevertheless, their number-based efficiencies were still acceptable (90.3 %, 86.3 % and 90.9 %, respectively).

3.1.2 Pressure Drop, Filtration Area, and Other Physical Properties

The pressure drops of the tested N95-EFs under 85 L/min flow rate varied largely from 25 to 185 Pa. As mentioned, pressure drop is very important and it depends on several physical properties including packing density, fiber diameter, thickness, and filtration area. As low as 50–65 Pa, samples 1, 4 and 5 passed both mass- and number-based 95 % efficiency, which was attributed to their high charging density (discussed later). Comparing samples 4 and 5, the latter had larger filtration area (23 % increase) and finer fiber diameter to compensate for its lower charging density. In general, the manufacturer intended to increase fiber charges to design their respirators with lower pressure drop for the comfort of the wearer. However, there is a high risk if the filter media is not properly charged when weighing and relying only on its low mechanical efficiency due to low pressure drop.

The filtration areas also varied largely from 143 to 235 cm^2. This means that the face velocity through the two extreme respirators had a 1.6 times difference, which can cause a nonnegligible filtration result. The differences in thickness, fiber diameter and solidity varied from 0.26 to 0.98 mm, 3.74 to 12.1 μm, and 0.091 to 0.195, respectively. The largest differences were 3.8, 3.2, and 2.1 times for these three parameters. Without considering their effectiveness, these randomly purchased N95-EFs had large differences in their physical design parameters. These unreasonably high differences were the potential reasons causing the failures of many respirators.

3.2 Empirical charging density

Once the required physical properties were obtained (**Table 1**), the charging density can be treated as the only variable in the theoretical FE calculation to match the experimental data. As expected, after applying favorable fiber charging density into the modeling, good agreements of whole size fractioned efficiency curve between theory (**Eqns. (3)–(19)** and **(22)–(23)**) and data were obtained for all samples. **Fig. 4** shows examples of the comparisons for 4 representative N95-EFs, including an N95 (#11), a KN95 (#17), a KF94 (#5), and an FFP2 (#9). It can be seen that the two curves almost collapsed together for all sizes, indicating that the applied charging density and the measured physical properties were very accurate.

3.2.1 MPPS and Charging Density

The charging density of the 30 samples varied from 2 to 122. The MPPS of filter media measured was closely related to the charging density and fiber diameter of the filter media (Chang et al., 2016; Tang et al., 2018a, b, c). When the media carried a relatively high charge, e.g., ≥50 μC/m^2, the MPPS would obviously move to small sizes, e.g., <50 nm. Our measurement results agreed with this trend.

Table 1 Specifications and test results of 30 commercial N95-EFs.

Label	Mass η	Number η at MPPS	MPPS (nm)	ΔP of whole mask (Pa)	ΔP of 4 cm flat sheet @10 cm/s (Pa)	Mask area (cm^2)	Thickness (mm)	The fiber diameter (μm)	Solidity	Charge density ($\mu C/m^2$)	Surface potential (V)	Std. ± (V)
1	0.998	0.985	29.4	50.0	75.0	212	0.98	10.2	0.135	122	1393.1	203.7
2	0.996	0.987	39.2	107.5	127.5	168	0.4	5.6	0.158	85	824.3	125.4
3	0.993	0.977	45.3	130.0	137.5	149	0.31	3.7	0.131	75	594.0	39.6
4	0.989	0.978	33.0	62.5	77.5	175	0.38	4.7	0.099	95	760.3	137.2
5	0.989	0.966	34.0	63.5	95.0	215	0.34	4.1	0.091	55	575.3	101.2
6	0.985	0.951	45.3	120.0	150.0	177	0.35	5.7	0.180	45	577.5	166.4
7	0.985	0.961	52.3	115.0	137.5	169	0.49	4.9	0.128	48	586.1	216.5
8	0.983	0.903	125.0	185.0	237.5	181	0.32	4.4	0.180	15	203.6	40.4
9	0.981	0.955	60.4	157.5	172.5	155	0.36	5.2	0.184	35	475.5	225.2
10	0.979	0.957	50.5	150.0	200.0	188	0.34	5.4	0.189	35	331.3	130.2
11	0.979	0.989	45.3	170.0	172.5	143	0.44	5.2	0.175	58	663.3	95.6
12	0.979	0.958	52.3	110.0	155.0	199	0.36	5.3	0.159	45	477.8	86.1
13	0.975	0.957	39.2	70.0	107.5	217	0.31	4.7	0.120	65	428.4	83.5
14	0.972	0.962	62.6	142.5	237.5	235	0.35	5.8	0.195	33	343.6	108.7
15	0.969	0.954	58.3	110.0	150.0	193	0.55	7.5	0.181	40	468.1	97.8
16	0.966	0.970	52.3	135.0	150.0	157	0.48	4.9	0.142	52	567.7	72.6
17	0.964	0.863	54.2	82.5	120.0	205	0.26	6.1	0.184	21	136.1	59.5
18	0.963	0.952	50.5	110.0	137.5	177	0.36	6.1	0.181	48	572.6	81.2
19	0.963	0.953	58.3	115.0	155.0	190	0.4	5.8	0.168	28	529.2	93.3
20	0.956	0.909	39.2	77.5	100.0	182	0.55	5.6	0.111	40	376.9	233.4
21	0.953	0.955	47.9	140.0	225.0	227	0.32	5.0	0.178	45	606.6	85.2
22	0.936	0.873	45.3	72.5	100.0	195	0.35	7.6	0.186	25	204.6	86.3
23	0.914	0.866	52.3	68.8	87.5	180	0.36	7.7	0.180	15	169.6	34.8
24	0.905	0.873	93.1	75.0	102.5	193	0.49	7.1	0.151	15	174.0	11.3
25	0.904	0.846	69.8	66.5	95.0	199	0.41	8.9	0.194	15	145.7	56.3
26	0.875	0.832	143.0	67.5	97.5	204	0.56	6.6	0.122	8.5	128.2	20.4
27	0.866	0.808	160.4	72.5	100.0	195	0.46	6.8	0.145	10	96.5	10.7
28	0.848	0.805	254.0	92.5	130.0	199	0.47	5.6	0.135	12	103.2	12.4
29	0.464	0.360	294.3	45.0	62.5	196	0.43	9.9	0.173	2	45.7	5.3
30	0.395	0.201	450.0	25.0	37.5	212	0.39	12.1	0.166	3	56.5	8.31

For example, the MPPSs were smaller than 40 nm for media with charges higher than 85 $\mu C/m^2$. The shifting of MPPS to small sizes is due to relatively large enhancement of deposition by fiber charge for larger particles than smaller ones. Both Coulombic and polarization attractions were almost negligible for particles smaller than ~50 nm due to relatively low carried and induced charges for small particles. On the contrary, when charging density smaller than ~10 $\mu C/m^2$, they could be treated as a mechanical filter. For example, samples 26–30 had relatively large MPPSs ranging 143–450 nm. It was speculated that the media were not successfully charged as expected or the rate of charge decay was too fast. As mentioned earlier, this is risky as these respirators relied mostly only on mechanical filtration, such as samples 29 and 30 had a relatively low efficiency of ~40 %.

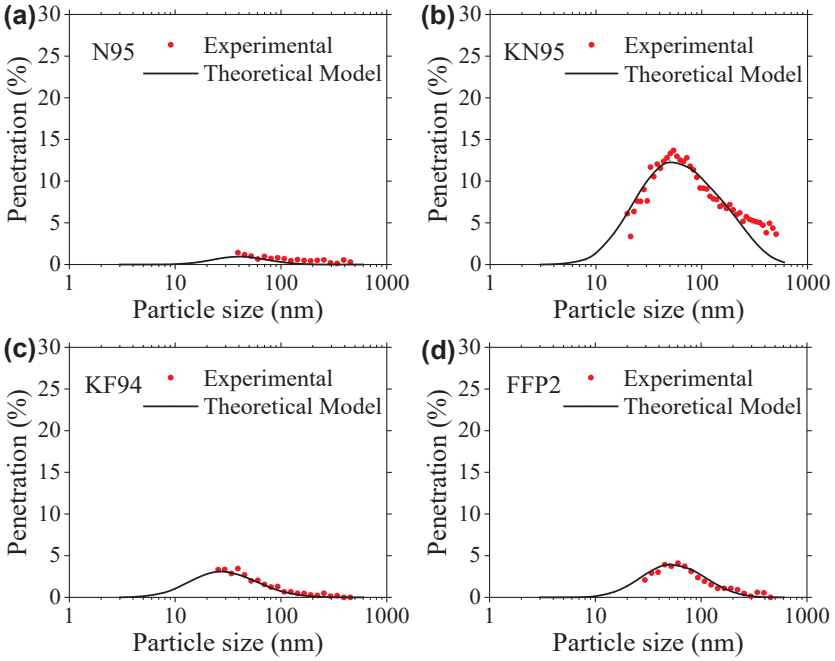

Fig. 4 Comparison of theoretical and experimental efficiency curve of sample 11 **(a)**, sample 17 **(b)**, sample 5 **(c)** and sample 9 **(d)** respirators.

3.2.2 Charging Density and Surface Potential

Table 1 also shows the measured surface potentials and standard deviations for the 30 samples. The surface potentials varied largely from 45.7 to 1393 and the deviations were not small, which majorly ranged ~10–40 % of the average potential. The surface potential is valid to be applied to the empirical equation only when it linearly correlates with the charging density. **Fig. 5** shows the comparison between the charge density and surface potential. A fairly good linear correlation with *R*-squared value of 0.906 was obtained. Therefore, this allowed us to substitute the charge density by the easily accessible surface potential to describe the charging property of filter media. This is a very important finding first reported, which was strictly based on rigorous experiments and theoretical calculations.

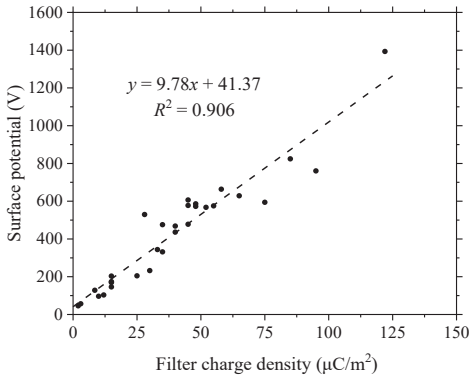

Fig. 5 Correlation of surface potential and charge density of tested respirators.

3.3 Empirical equation for the FE of MPPS

Now the final step toward the applicability of the empirical equation involving only pressure drop, filtration area and surface potential to predict the efficiency of MPPS is to compare the prediction to the experimental data. Again, the three parameters are relatively easy to obtain as described earlier. Preferably, penetration may be used in the empirical equation as it was the first calculation result (**Eqn. (17)**) in the modeling. However, to have an intuitive relation with the 95 % FE of N95-EFs, we chose to use efficiency in the equation. There are many commercially available fitting programs, and we used TableCurve 3D software (Systat Software Inc., San Jose, CA) to find the equation.

When all three parameters are applied, there will be 3 independent and 1 dependent variables, which are one dimension over what the software can do. So, we combined the pressure drop and surface area by multiplying them together. This is reasonable as the FE increases with both parameters. Further, to make each term of the variable in the equation dimensionless, the reference pressure drop, respirator area, and surface potential should be determined. Ideally, the parameters from a standard filter media should be used. However, it is not available for now and has to be developed in the near future. We thus tried using a NIOSH certified N95, i.e. sample 11, as the reference.

The developed equation was a curved surface having a format of:

$$\eta_{\mathrm{MPPS,p}} = a + b\ln x + c(\ln x)^2 + d(\ln x)^3 + e\ln y \qquad (24)$$

where $a = 1.0036$, $b = -0.01725$, $c = 0.09753$, $d = 0.18983$, $e = -0.03338$, $R^2 = 0.966$, $\eta_{\mathrm{MPPS,p}}$ is the predicted FE of MPPS, x is the normalized product of the pressure drop and respirator area ($x = (\Delta P{\cdot}S)_{\mathrm{sample}}/(\Delta P{\cdot}S)_{\mathrm{N95}}$), and y is the

normalized surface potential ($y = V_{sample}/V_{N95}$). The comparison between measured and predicted FE at MPPS for the 30 samples is shown in **Table 2**. With a good *R*-squared value of 0.966, it can be seen that the predicted FEs (η predicted) by the empirical equation are less than 8 % (majorly less than ~3 %) difference from the experimental FEs (η data). The equation is very reliable because its prediction is accurate in distinguishing whether the samples pass or fail 95 % FE. For example, the equation would not predict a pass if the data showed fail and vice versa. The only exceptions were sample 10 and 20. The empirical equation underestimated the FE of sample 10 for about 2 %, and overestimated that of sample 20 for about 5 %. Therefore, we believe that the accuracy of the equation can be further improved by adding more data. Typically, we should have more mechanical respirators and those respirators that have FE around 95 % to comprehend the equation.

3.4 Validation and application of the developed empirical equation

It is very meaningful to validate the accuracy and

Table 2 Comparison of the predicted efficiency by the empirical equation model with the experimental efficiency.

Label	*x*	*y*	η, data	η, predicted	Residual
1	0.435	2.100	0.9849	0.9601	–0.0248
2	0.739	1.243	0.9867	0.9857	–0.0010
3	0.797	0.896	0.9766	0.9731	–0.0035
4	0.449	1.146	0.9781	0.9535	–0.0246
5	0.551	0.867	0.9655	0.9699	0.0044
6	0.870	0.871	0.9513	0.9691	0.0178
7	0.797	0.884	0.9605	0.9726	0.0121
8	1.377	0.307	0.9033	0.9056	0.0023
9	1.000	0.717	0.9546	0.9571	0.0025
10	1.160	0.500	0.9569	0.9370	–0.0199
11	1.000	1.000	0.9893	0.9703	–0.0190
12	0.899	0.720	0.9575	0.9600	0.0025
13	0.623	0.646	0.9570	0.9619	0.0049
14	1.377	0.518	0.9624	0.9500	–0.0125
15	0.870	0.706	0.9540	0.9601	0.0061
16	0.870	0.856	0.9704	0.9684	–0.0020
17	0.696	0.205	0.8631	0.8510	0.0103
18	0.797	0.863	0.9516	0.9717	0.0201
19	0.899	0.798	0.9533	0.9645	0.0112
20	0.580	0.568	0.9087	0.9525	0.0438
21	1.304	0.915	0.9549	0.9730	0.0181
22	0.580	0.308	0.8727	0.9030	0.0303
23	0.507	0.256	0.8663	0.8704	0.0041
24	0.594	0.262	0.8727	0.8851	0.0124
25	0.551	0.220	0.8458	0.8564	0.0106
26	0.565	0.193	0.8315	0.8373	0.0058
27	0.580	0.146	0.8078	0.7820	–0.0258
28	0.754	0.156	0.8053	0.7976	–0.0077
29	0.362	0.069	0.3600	0.4387	0.0787
30	0.217	0.085	0.2013	0.1905	–0.0108

feasibility of the equation. So, we use extra 5 new samples to test the equation. **Table 3** summarizes the pressure drop, filtration area, surface potential, and measured and predicted MPPS FE. Results showed that the maximum difference between data and prediction was only 3.4 %. Therefore, it is to conclude that the empirical equation is easy to use and can be applied to predict the MPPS FE.

3.5 Application of the developed empirical equation

The developed empirical equation **Eqn. (24)** was applied to help redesign the mechanical filters that were examined and did not pass 95 % MPPS FEs. Samples 8, 26, 28, 29 and 30 (see **Table 1**) were selected as representative mechanical respirators. By keeping the filtration area and surface potential unchanged, the equation was able to find the pressure drop required to improve them to have an MPPS FE larger than 95 %. The pressure drop required to be increased (or adding, e.g., through adding thickness) are summarized in **Table 4**. Sample 8 only needed 52.1 Pa to increase its MPPS FE from 90.3 % to 95 %, but others needed more (~180–360 Pa) as their original FEs were lower (~0.2–0.83). Comparing the calculation results between samples 29 and 30, a lower adding of pressure drop was needed for Sample 30 even its original FE was lower. This was attributed to the larger size of MPPS for sample 30 (450 nm) than 29 (294 nm). This indicated that **Eqn. (24)** with the feeds of data from 30 respirators is smart enough to consider the size effect in the filtration mechanism. One can also use **Eqn. (24)** to find the required filtration area or surface potential (or charging density) for these mechanical respirators to pass 95 % MPPS FE. Ultimately, the equation also allows users to adjust all three main parameters at the same time to design a good N95-EF with low pressure drop or low quantity of filter media. However, to note, **Eqn. (24)** is applicable to predict the MPPS FE for the respirators with specifications falling inside the boundary of the 30 samples. That is, it is limited to pressure drop from 25 to 185 Pa, filtration area of 143–235 cm^2 and surface potential of 46–1393 V.

4. Conclusion

To determine whether an N95 Equivalent-Facepiece filtering respirator (N95-EF) has passed 95 % filtration efficiency (FE), either through experimental measurement or theoretical calculation, is complex and cumbersome. This complexity could be the major reason causing the high failure rate for N95-EF sold in the market at the beginning of the COVID-19 pandemic, as respirator manufacturers could not easily follow the standard protocols to control their quality. In this study, we proposed a simple method to qualify commercial N95-EFs. It was based on rigorous empirical evidence and theoretical calculations. Specifically, we utilized three important and easily accessible respirator parameters including pressure drop, filtration area, and surface potential to form an empirical equation to predict FE at the most penetrating particle size (MPPS). Notably, The surface potential well correlated with the charging density, so it was used as its substitute. To note, the equation is reliable only if these parameters are defined correctly.

In the development of the empirical equation, we first built a standard test rig based on Chinese Standard GB 2626 to perform both mass- and number-based efficiency

Table 3 Validation of the developed empirical equation for 5 new masks.

New Sample	ΔP (Pa)	Area (cm^2)	Average surface potential (V)	Measured η at MPPS	Predicted η at MPPS	Residual
A	67.5	204	142.1	0.830	0.857	–0.027
B	72.5	200	175.5	0.866	0.877	–0.011
C	170	145	750.1	0.984	0.971	–0.013
D	110	199	477.3	0.958	0.950	–0.008
E	82.5	193	167.4	0.841	0.875	0.034

Table 4 Empirical equation application for mechanical filters.

Label	Mass η	Number η at MPPS	MPPS	ΔP (Pa)	Surface area (cm^2)	Surface potential (V)	Required η at MPPS	Predicted ΔP (Pa)	ΔP adding (Pa)
8	0.983	0.903	125	185	181	203.6	0.95	236.2	52.1
26	0.875	0.832	143	67.5	204	128.2	0.95	251.4	183.9
28	0.848	0.805	254	92.5	199	89.4	0.95	298.1	205.6
29	0.464	0.361	294	45.0	196	45.7	0.95	405.6	360.6
30	0.395	0.201	450	25.0	212	56.5	0.95	340.7	315.7

evaluation of 35 different commercial N95-EFs. In addition, all respirators were measured with their thickness, fiber size, packing density, surface potential, and filtration area. The surface potential was correlated with the charge density derived through the comparison between the experimental and theoretical efficiency. Findings demonstrated a good correlation between filter charge density and surface potential validating the substitution.

The prediction of MPPS FE by the equation was accurate and majorly (28 out of 30) with ≤3 % of efficiency difference from the data. The empirical equation was successfully validated by comparing it with data from additional 5 new samples. The empirical equation was also successfully applied to help redesign mechanical respirators. To conclude, this work provides a simple empirical equation for quickly qualifying FEs of respirators. The equation can also be applied to design N95-EFs.

In conclusion, this study presents a straightforward empirical equation for rapidly assessing the filtration efficiencies of respirators, which can also guide N95-EF design. The equation is powerful but for now it is applicable to the respirators with specifications falling inside the boundary of the 30 samples tested. It is limited to pressure drop from 25 to 185 Pa, filtration area of 143–235 cm^2 and surface potential of 46–1393 V. To further improve the accuracy of the equation, more respirators should be tested, and their data should be included in refining the empirical equation.

Data Availability Statement

The data have been included in **Tables 1–4** and the row data are available upon request.

Acknowledgments

This work was financially supported by the Center for Filtration Research (CFR) at the University of Minnesota. The authors thank the CFR members including 3M, Applied Materials, BASF, Boeing Company, China Yancheng Environmental Protection Science and Technology City, Cummins Filtration, Donaldson Company, Ford Motor Company, Freudenberg Group, Guangxi Wat Yuan Filtration System, Mann Hummel GmbH, Math2Market GmbH, Samsung Electronics, Parker-Hannifin, Shigematsu Works, TSI, W. L. Gore & Associates, Xinxiang Shengda Filtration Technique.

Nomenclature

FE	Filtration efficiency
FFR	Facepiece filtering respirator
GSD	Geometric standard deviation
MPPS	Most penetrating particle size
NMD	Number median diameter
NIOSH	National Institute for Occupational Safety and Health
GB	National Standards of the People's Republic of China
N95-EF	N95 equivalent facepiece filtering respirator
A	Surface area
C_c	Cunningham slip correction factor
$C_{m,up}$	Upstream mass concentration
$C_{m,down}$	Downstream mass concentration
$C_{n,up}$	Upstream number concentration
$C_{n,down}$	Downstream number concentration
C_p	Capacitance of the capacitor
D	Diffusion coefficient
d_f	Fiber diameter in the filter media
d_x	Particle diameter
E_T	Total single fiber efficiency
E_D	Partial diffusion efficiency
E_R	Partial interception efficiency
E_{DR}	Partial efficiency for interception of diffusing particles
E_I	Partial impaction efficiency
E_q	Partial electrostatic deposition efficiency
E_{qC}	Depositions by the Coulomb force
E_{qD}	Depositions by the dielectric polarization force
Ku	Kuwabara hydrodynamic parameter
N_{CD}	Dimensionless parameter for charged particles through bipolarly charged fibrous filter media
N_{DD}	Dimensionless parameter for uncharged particles through bipolarly charged fibrous filter media
Pe	Peclet number
$P_{largest,\ dx}$	Largest size dependent penetration
$P_{theo,\ dx}$	Theoretical particle penetration
$P1$	Measured pressure drop of the whole respirator
$P2$	Measured pressure drop of the 4 cm circular sheet
$q(n)$	Carried charges of the particle (C)
Q	Charge carried by the sample surface
R	The ratio of particle diameter to fiber diameter
Stk	Stokes number
t	The thickness of sample
U_0	Face velocity (cm/s)
V	Measured surface potential
V_p	The potential of the voltmeter probe
W	Weight of the flat sheet (g)
x	Normalized product of pressure drop and mask area
y	Normalized surface potential
α	Solidity
ε_d	The permittivity of the sample between the electrode and the tested surface
ε_f	Fabric dielectric constant
ε_p	The relative permittivity of the particle
ε_0	The permittivity of the vacuum (8.85×10^{-12} $C^2/N \cdot m^2$)
$\eta_{theo,dx}$	Theoretical filtration efficiency
η_m	Mass-based filtration efficiency
η_{MPPS}	Number-based minimum efficiency
$\eta_{MPPS,p}$	Predicted number-based minimum efficiency
μ	Air viscosity ($N \cdot s/m^2$)
ρ_f	The density of filter media (g/cm^3)
ρ_p	Particle density (2.2 g/cm^3 here)
σ	Charge density (C/m^2)

References

Antoniu A., Dascalescu L., Vacar I.-V., Plopeanu M.-C., Tabti B., Teodorescu H.-N.L., Surface potential versus electric field measurements used to characterize the charging state of nonwoven fabrics, IEEE Transactions on Industry Applications, 47 (2011) 1118–1125. https://doi.org/10.1109/TIA.2011.2127432

Bahk J.-H., Bian Z., Shakouri A., Electron energy filtering by a nonplanar potential to enhance the thermoelectric power factor in bulk materials, Physical Review B, 87 (2013) 075204. https://doi.org/10.1103/PhysRevB.87.075204

Balazy A., Toivola M., Reponen T., Podgorski A., Zimmer A., Grinshpun

S.A., Manikin-based performance evaluation of N95 filtering-facepiece respirators challenged with nanoparticles, The Annual Occupational Hygiene, 50 (2006) 259–269. https://doi.org/10.1093/annhyg/mei058

Cai C., Floyd E.L., Effects of sterilization with hydrogen peroxide and chlorine dioxide solution on the filtration efficiency of N95, KN95, and surgical face masks, JAMA Network Open, 3 (2020) e2012099. https://doi.org/10.1001/jamanetworkopen.2020.12099

Chang D.-Q., Chen S.-C., Fox A.R., Viner A.S., Pui D.Y.H., Penetration of sub-50 nm nanoparticles through electret HVAC filters used in residence, Aerosol Science and Technology, 49 (2015) 966–976. https://doi.org/10.1080/02786826.2015.1086723

Chang D.-Q., Chen S.-C., Pui D.Y.H., Capture of sub-500 nm particles using residential electret HVAC filter media-experiments and modeling, Aerosol and Air Quality Research, 16 (2016) 3349–3357. https://doi.org/10.4209/aaqr.2016.10.0437

Chang D.-Q., Liu J.-X., Chen S.-C., Factors affecting particle depositions on electret filters used in residential HVAC systems and indoor air cleaners, Aerosol And Air Quality Research, 18 (2018) 3211–3219. https://doi.org/10.4209/aaqr.2018.10.0373

Chen C., Zhao B., Zhou W., Jiang X., Tan Z., A methodology for predicting particle penetration factor through cracks of windows and doors for actual engineering application, Building and Environment, 47 (2012) 339–348. https://doi.org/10.1016/j.buildenv.2011.07.004

Chen S.-C., Wang J., Bahk Y.-K., Fissan H., Pui D.Y.H., Carbon nanotube penetration through fiberglass and electret respirator filter and Nuclepore filter media: experiments and models, Aerosol Science and Technology, 48 (2014) 997–1008. https://doi.org/10.1080/02786826.2014.954028

CDC (Centers for Disease Control and Prevention), 2020. Types of masks and respirators <www.cdc.gov/coronavirus/2019-ncov/prevent-getting-sick/types-of-masks.html> accessed 29.01.2022.

CDC (Centers for Disease Control and Prevention), 2021, Use of masks to control the spread (COVID-19) <www.cdc.gov/coronavirus/2019-ncov/science/science-briefs/masking-science-sars-cov2.html> accessed 29.01.2022.

Davies C.N., Diffusion and sedimentation of aerosol particles from Poiseuille flow in pipes, Journal of Aerosol Science, 4 (1973) 317–328. https://doi.org/10.1016/0021-8502(73)90092-X

Dhand R., Li J., Coughs and sneezes: their role in transmission of respiratory viral infections, including SARS-CoV-2, American Journal of Respiratory and Critical Care Medicine, 202 (2020) 651–659. https://doi.org/10.1164/rccm.202004-1263PP

Duncan S., Bodurtha P., Naqvi S., The protective performance of reusable cloth face masks, disposable procedure masks, KN95 masks and N95 respirators: filtration and total inward leakage, PLOS ONE, 16 (2021) e0258191. https://doi.org/10.1371/journal.pone.0258191

Forsyth B., Liu, B.Y.H., Romay, F.J., Particle charge distribution measurement for commonly generated laboratory aerosols, Aerosol Science and Technology, 28 (1998) 489–501. https://doi.org/10.1080/02786829808965540

GB 2626, Respiratory protective equipment—non-powered air-purifying particle respirator, National Standard of the People's Republic of China, 2006.

Hao J., Passos De Oliveira Santos R., Rutledge G.C., Examination of nanoparticle filtration by filtering facepiece respirators during the COVID-19 pandemic, ACS Applied Nano Materials, 4 (2021) 3675–3685. https://doi.org/10.1021/acsanm.1c00139

Hinds W.C., Aerosol Technology: Properties, Behavior, and Measurement of Airborne Particles, 2nd ed., J. Wiley, New York, 1999, ISBN: 0-471-19410-7.

Jayaweera M., Perera H., Gunawardana B., Manatunge J., Transmission of COVID-19 virus by droplets and aerosols: a critical review on the unresolved dichotomy, Environmental Research, 188 (2020) 109819. https://doi.org/10.1016/j.envres.2020.109819

Kachi M., Nemamcha M., Tabti B., Dascalescu L., Comparison between three measurement methods for characterizing the charge state of granular insulating materials, Journal of Electrostatics, 69 (2011) 394–400. https://doi.org/10.1016/j.elstat.2011.05.002

Liu Z., Chen D.-R., Niu Q., Mensah D.A., Ji Z., Particle collection of electret media under different filtration pressures, Aerosol and Air Quality Research, 23 (2023) 220405. https://doi.org/10.4209/aaqr.220405

Patra I., Huy D.T.N., Alsaikhan F., Opulencia M.J.C., Van Tuan P., Nurmatova K.C., Majdi A., Shoukat S., Yasin G., Margiana R., Walker T.R., Karbalaei S., Toxic effects on enzymatic activity, gene expression and histopathological biomarkers in organisms exposed to microplastics and nanoplastics: a review, Environmental Sciences Europe, 34 (2022) 80. https://doi.org/10.1186/s12302-022-00652-w

Plana D., Tian E., Cramer A.K., Yang H., Carmack M.M., Sinha M.S., Bourgeois F.T., Yu S.H., Masse P., Boyer J., Kim M., Mo J., LeBoeuf N.R., Li J., Sorger P.K., Assessing the filtration efficiency and regulatory status of N95s and nontraditional filtering face-piece respirators available during the COVID-19 pandemic, BMC Infectious Diseases, 21 (2021) 712. https://doi.org/10.1186/s12879-021-06008-8

Prather K.A., Wang C.C., Schooley R.T., Reducing transmission of SARS-CoV-2, Science, 368 (2020) 1422–1424. https://doi.org/10.1126/science.abc6197

Sachinidou P., Heuschling C., Schaniel J., Wang J., Investigation of surface potential discharge mechanism and kinetics in dielectrics exposed to different organic solvents, Polymer, 145 (2018) 447–453. https://doi.org/10.1016/j.polymer.2018.05.023

Schilling K., Gentner D.R., Wilen L., Medina A., Buehler C., Perez-Lorenzo L.J., Pollitt K.J.G., Bergemann R., Bernardo N., Peccia J., Wilczynski V., Lattanza L., An accessible method for screening aerosol filtration identifies poor-performing commercial masks and respirators, Journal of Exposure Science & Environmental Epidemiology, 31 (2021) 943–952. https://doi.org/10.1038/s41370-020-0258-7

Stahl C., Frederick K., Chaudhary S., Morton C.J., Loy D., Muralidharan K., Sorooshian A., Parthasarathy S., Comparison of the filtration efficiency of different face masks against aerosols, Frontiers in Medicine, 8 (2021) 654317. https://doi.org/10.3389/fmed.2021.654317

Tang M., Chen S.-C., Chang D.-Q., Xie X., Sun J., Pui D.Y.H., Filtration efficiency and loading characteristics of $PM_{2.5}$ through composite filter media consisting of commercial HVAC electret media and nanofiber layer, Separation and Purification Technology, 198 (2018a) 137–145. https://doi.org/10.1016/j.seppur.2017.03.040

Tang M., Thompson D., Chen S.-C., Chang D.-Q., Pui D.Y.H., Filtration efficiency and loading characteristics of $PM_{2.5}$ through commercial electret filter media, Separation and Purification Technology, 195 (2018b) 101–109. https://doi.org/10.1016/j.seppur.2017.11.067

Tang M., Thompson D., Chen S.-C., Liang Y., Pui D.Y.H., Evaluation of different discharging methods on HVAC electret filter media, Building Environment, 141 (2018c) 206–214. https://doi.org/10.1016/j.buildenv.2018.05.048

Tien C.Y., Chen J.P., Li S., Li Z., Zheng Y.M., Peng A.S., Zhou F., Tsai C.-J., Chen S.-C., Experimental and theoretical analysis of loading characteristics of different electret media with various properties toward the design of ideal depth filtration for nanoparticles and fine particles, Separation and Purification Technology, 233 (2020) 116002. https://doi.org/10.1016/j.seppur.2019.116002

Wang J., Chen D.R., Pui D.Y.H., Modeling of filtration efficiency of nanoparticles in standard filter media, Journal of Nanoparticle Research, 9 (2007) 109–115. https://doi.org/10.1007/s11051-006-9155-9

Wang J., Kim S.C., Pui D.Y.H., Measurement of multi-wall carbon nanotube penetration through a screen filter and single-fiber analysis, Journal of Nanoparticle Research, 13 (2011) 4565–4573. https://doi.org/10.1007/s11051-011-0415-y

Yan Y., Zhou X., Xu H., Melcher K., Structure and physiological regulation of AMPK, International Journal of Molecular Sciences, 19 (2018) 3534. https://doi.org/10.3390/ijms19113534

You R., Zhao B., Chen C., Developing an empirical equation for modeling particle deposition velocity onto inclined surfaces in indoor environments, Aerosol Science and Technology, 46 (2012) 1090–1099. https://doi.org/10.1080/02786826.2012.695096

Authors' Short Biographies

Dr. Sheng-Chieh Chen is an Associate Professor in the Department of Mechanical and Nuclear Engineering at Virginia Commonwealth University. He has been working on research on aerosol science and technology for about 2 decades. Air filtration is his current focus, typically for charged filter media used in respirators, HVAC systems, and indoor air purifiers.

Dr. Yu Zhang was trained as a Mechanical Engineer. She received her PhD degree from the Department of Mechanical and Nuclear Engineering at Virginia Commonwealth University in April 2023. Her expertise is in indoor air pollutants control. She fabricated photocatalytic metal-organic framework (MOF) coated electret which can simultaneously remove particulate matters (PMs), volatile organic compounds (VOCs), and bioaerosol.

Mr. Genhui Jing is a PhD student in the Department of Mechanical and Nuclear Engineering at Virginia Commonwealth University. He received his master's degree from the College of Chemistry & Chemical Engineering, Xi'an Shiyou University. He is studying nanoparticle removal by air and liquid filtration.

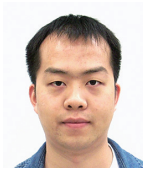

Dr. Peng Wang was trained as a Mechanical Engineer. He received his PhD degree from the Department of Mechanical and Nuclear Engineering at Virginia Commonwealth University in August 2021. His expertise is in experimental and numerical study of air filtration.

Prof. Daren-Chen is a Professor and Floyd D. Gottwald, Sr. Chair in the Department of Mechanical and Nuclear Engineering at Virginia Commonwealth University. He is the inventor of many aerosol generation and measurement instruments, including electrospray monodisperse particle generator, nanometer differential mobility analyzer, personal nanoparticle monitors, continuous gene transfection and many other particle processing tools. He was honored with the Sheldon K. Friedlander Award (1997), Smoluchowski Award (2002), Kenneth Whitby Award (2005) and Benjamin Liu Award (2012) for his significant contributions to nanoparticle instrumentation and experimental techniques.